npj | science of learning

Article

Published in partnership with The University of Queensland

Article in Press

https://doi.org/10.1038/s41539-026-00452-4

Learning environments are associated with age-related differences in thalamocortical attention circuits in childhood

Check for updates

Tamara Mino-Matot[1,2,5], Hamza Kebiri[1,3,5], João Jorge[4], Jean-Baptiste Ledoux[1,3], Eleonora Fornari[1,3], Meritxell Bach Cuadra[1,3] & Solange Denervaud[1,2]

The thalamus plays a central role in sensory gating and large-scale cortical communication, but its developmental organization in relation to real-world learning environments has rarely been examined. Here, we analyzed resting-state fMRI data from 72 children aged 4–15 years enrolled in Montessori or traditional classrooms. Using a data-driven parcellation approach based on voxelwise functional connectivity, we identified five spatially coherent thalamic territories with distinct large-scale connectivity profiles, primarily linked to visual, sensorimotor, and attention networks. In a thalamic territory preferentially coupled to the ventral attention system, Montessori enrollment was associated with stronger thalamocortical connectivity and a stronger positive association between age and FC. No clusters showed enhanced connectivity with executive-control or default-mode networks, consistent with their later maturation. Together, these findings suggest that schooling context co-varies with the developmental refinement of thalamic circuits supporting salience detection and the selective prioritization of information during learning. Because the design is cross-sectional and families self-select into schools, causal direction cannot be inferred and unmeasured family-level factors (e.g., parental values, home learning environment) may contribute to these associations. Nonetheless, the results identify a tractable neural pathway through which everyday learning environments may relate to developing brain systems underlying attention and adaptive behaviour.

The thalamus is a central regulator of cortical computation in development, shaping how information is prioritized, routed, and sustained across large-scale networks[1,2]. Rather than a passive relay, thalamic circuits dynamically gate sensory and cortico-cortical signals, supporting the emergence of executive control, goal-directed behavior, and sustained attention. These channels are present early, yet undergo protracted refinement through childhood and adolescence, tracking the maturation of higher-order cognition[3,4]. This maturational window coincides with the school years, i.e., an intensive, socially embedded context with distinct attentional demands, sensory contingencies, and autonomy structures, yet links between everyday pedagogy and thalamocortical organization remain unclear. Given the thalamus's role in sensory integration and attentional gating[5,6], its connectivity may be especially sensitive to practices that differentially emphasize self-paced exploration (e.g., Montessori education) versus externally imposed structure (e.g., traditional education), see comparative details in Table S9.

Anatomically, the thalamus comprises multiple nuclei with distinct projections to cortex, subcortex, and cerebellum[4], including First-Order relays and Higher-Order nuclei that mediate cortico-cortical communication[6,7]. This architecture is sculpted by the thalamic reticular nucleus (TRN) and by cerebello-basal ganglia loops[2,8], enabling coordination of sensorimotor processing, learning, memory consolidation, and cognitive control[9,10]. Perturbations to these circuits carry developmental costs in both animal models and humans, implicating thalamic organization

[1]CIBM Center for Biomedical Imaging, Lausanne, Switzerland. [2]MRI imaging and technology, Polytechnical School of Lausanne, Swiss Federal Institute of Technology Lausanne (EPFL), Lausanne, Switzerland. [3]Department of Radiology, Lausanne University Hospital and University of Lausanne (CHUV-UNIL), Lausanne, Switzerland. [4]CSEM – Swiss Center for Electronics and Microtechnology, Bern, Switzerland. [5]These authors contributed equally: Tamara Mino-Matot, Hamza Kebiri. e-mail: solange.denervaud@epfl.ch

Table 1 | Behavioral and Demographic Characteristics of the Study Sample

Variable	Traditional (n = 40)	Montessori (n = 32)	Test statistic	p
Age (years), M (SD)	10.20 (2.60)	9.26 (2.51)	t(67.5) = 1.56	0.123
Gender, n (Male / Female)	26 / 14	17 / 15	$\chi^2(1) = 1.04$	0.307
Fluid intelligence, M (SD) (Raven's Progressive Matrices, raw score)	33.10 (3.08)	32.44 (4.59)	t(52.3) = 0.70	0.486
Socioeconomic status, M (SD) (IPSE index)	3.08 (0.62)	3.03 (0.46)	t(68.9) = 0.36	0.722
Years in current school, M (SD)	2.61 (1.43)	2.35 (1.20)	t(68.5) = 0.82	0.414
Age at school entry (years), M (SD)	7.60 (3.28)	6.95 (2.56)	t(69.0) = 0.93	0.358

Continuous variables are summarized as mean (standard deviation). Welch's t-test was used to allow for unequal variances between groups; df therefore is non-integer. Fluid intelligence was measured with the Raven's Coloured / Standard Progressive Matrices (PM47), raw score[37]. Socioeconomic status (SES) was indexed using the Indice de position socio-économique (IPSE; ref. 38). Years in current school and age at school entry were derived from the parental questionnaire; missing for one Montessori-enrolled child.
Demographic and cognitive measures are presented for children enrolled in Montessori and traditional school settings. *SES* socioeconomic status, *SD* stands for standard deviation.

as a bottleneck for downstream cognition: TRN disruption produces hyperactivity and attentional dysregulation in rodents[8,11], and atypical thalamic structure/connectivity is associated with dyslexia, ADHD, and learning difficulties in humans[12,13]. Converging evidence also indicates that higher-order thalamic nuclei (e.g., pulvinar, mediodorsal) modulate inter-areal communication during attention and learning[14], and that thalamo-cortical coupling shows experience-related reweighting across development[3]. Within this framework, schooling contexts that differentially engage attentional, memory, and sensorimotor demands, such as Montessori's multisensory, embodied, child-led approach[15], are associated with enhancements in multisensory integration, semantic memory, creativity, and functional stability in attention and sensorimotor networks[16–18], motivating the hypothesis that pedagogy may be associated with distinct thalamic connectivity profiles during development.

Progress on experience-related differences has been limited by methods that transfer adult atlases to children and may obscure age-specific thalamic heterogeneity. We therefore adopt a pediatric, data-driven functional parcellation of the thalamus for resting-state fMRI, allowing the data to determine parcel boundaries. Building on an infant-derived k-means framework (KNIT; ref. 19), we (i) derive voxelwise thalamus-to–parcel connectivity by correlating each thalamic voxel with parcel-wise mean time series from 508 brain regions (cortex + subcortex; Lausanne2018 atlas), using a child-optimized acquisition and robust preprocessing; (ii) allow the data to determine the number and boundaries of thalamic territories via an a priori multi-granularity search over K with objective selection criteria (spatial coherence, hemispheric symmetry, functional specificity); and (iii) link each subregion's large-scale "fingerprint" to behaviorally relevant context via cluster-resolved modeling of pedagogy, age, and gender with multiple-comparison control. This approach moves beyond adult-atlas transfer and yields an empirically grounded map of pediatric thalamic organization suitable for testing experience-related hypotheses.

We analyzed high-temporal resolution resting-state fMRI from children aged 4–15 years enrolled in Montessori or traditional schools. Using the pediatric-adapted KNIT pipeline, we test three hypotheses: (1) the pediatric thalamus can be robustly and interpretably subdivided using data-driven clustering; (2) thalamocortical profiles differ by schooling context in a demographically matched sample; and (3) age tracks shift in connectivity consistent with known developmental trajectories.

Results

Behavioral measures and demographics

Demographic and behavioral data are summarized in Table 1. No significant differences were observed between children enrolled in Montessori versus traditional school systems with respect to gender distribution, chronological age, fluid intelligence, or socioeconomic status (all $p > 0.12$), indicating a matched sample across groups.

Thalamic clustering procedure using KNIT model

Thalamic functional parcellation was first conducted across the full sample using k-means clustering. Across $K = 3$ to $K = 15$, the Calinski–Harabasz index peaked at $K = 8$ and the Davies–Bouldin index reached a local minimum at $K = 8$ (Fig. S5), while the silhouette coefficient was highest at $K = 6$ (Fig. S5; see also Fig. S2 and Fig. S4 for the corresponding spatial segmentations at $K = 6$ and $K = 8$). The in-between $K = 7$ solution (Fig. S3) yielded seven distinct clusters, two of which (Clusters 1 and 2 of $K = 7$) were excluded due to low voxel count (< 35 voxels), and one further cluster (Cluster 5 of $K = 7$) displayed poor spatial coherence (scattered and asymmetrical across hemispheres). At $K = 6$, two clusters fell below the a priori 60-voxel threshold (see Methods), reducing the effective parcellation to four interpretable territories. At $K = 8$ (Fig. S4), the segmentation reproduced the major connectivity patterns observed at $K = 6$ (that showed one of the best silhouette scores) with the addition of a distinct (eighth) territory contributing further specificity. Based on spatial compactness, hemispheric symmetry ($K = 8$ exhibited the highest ARI of 0.222, exceeding all lower-K solutions), and functional distinctiveness, and after considering the quantitative metrics, the $K = 8$ solution was retained for all subsequent analyses (Fig. 1). Three of the eight $K = 8$ clusters were not retained for functional connectivity analyses: $K = 8$ Clusters 3 and 6 fell below the a priori 60-voxel exclusion threshold and were considered noise; $K = 8$ Cluster 7 (108 voxels) appeared visually scattered and asymmetric and was similarly excluded. Sensitivity analyses re-including these three clusters did not alter the pattern of Pedagogy and Pedagogy × Age effects in the five retained territories (Suppl. Table S4).

Cluster validation and network characterization

In the $K = 8$ solution, five thalamic cluster exhibited a distinct and interpretable functional connectivity profile with large-scale brain networks (Fig. 1C). Cluster 1 showed strong positive connectivity with the visual network and strong negative connectivity with the limbic system, suggesting a role in sensory filtering or visual-limbic dissociation. Clusters 2 and 5 demonstrated robust connectivity with both subcortical structures and the ventral attention network, indicative of integrated thalamo-cortical involvement in salience detection and attentional control. Notably, Cluster 2 displayed anti-correlated activity with the dorsal attention system. Cluster 5 exhibited concurrent anti-correlations with both the visual and limbic networks, reflecting a potentially distinct regulatory role in balancing external sensory and internal emotional inputs. Finally, Cluster 4 showed preferential connectivity with the somatomotor and dorsal attention networks, along with negative correlations with limbic regions, suggesting a sensorimotor-attentional integration pathway modulated by affective gating.

Functional connectivity analyses

For Cluster 2, a significant main effect of Pedagogy was observed, $F(1, 66) = 8.26$, $p = 0.005$, pFDR-within-cluster = 0.027 (pFDR across all 25

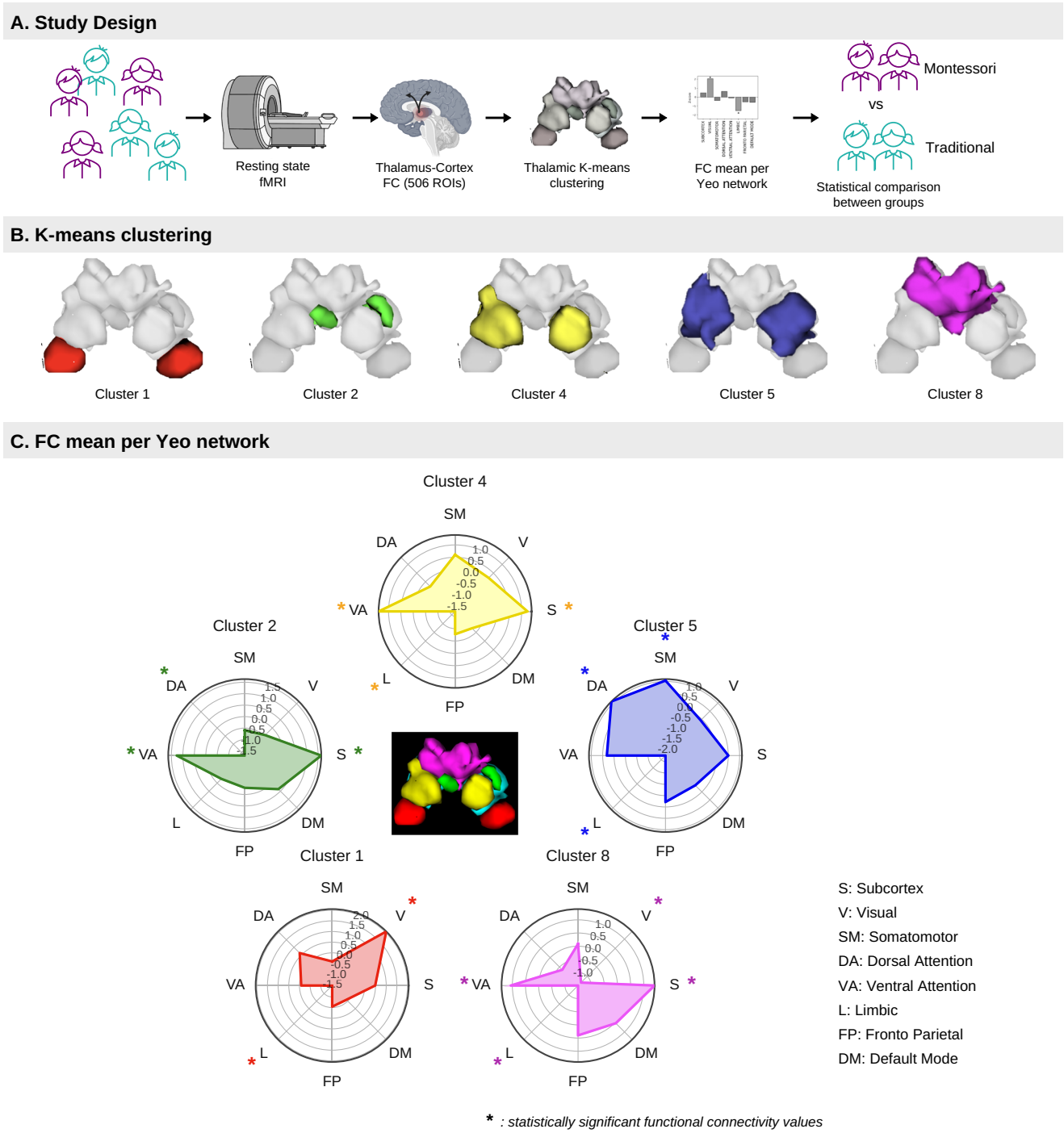


Fig. 1 | A Study Design. Diagram illustrating from left to right the different steps of the study protocol. **B** Functional Segmentation of the Thalamus Using $K = 8$ Clustering Across the Full Cohort. This panel shows the eight thalamic clusters identified through k-means clustering and their spatial distribution within the thalamus, presented as a 3D rendering. Five clusters (numbers 1, 2, 4, 5, and 8) met the criteria of spatial compactness, hemispheric symmetry, and functional distinctiveness and were used for the subsequent functional connectivity analyses. Clusters 3, 6, and 7 were discarded (clusters 3 and 6 below the 60-voxel threshold; cluster 7 spatially scattered and asymmetric). **C** Functional Connectivity Profiles of the five retained Thalamic Clusters from the $K = 8$ Segmentation. Each plot depicts the z-scored functional connectivity (FC) values for each of the five thalamic clusters across the seven canonical Yeo cortical networks and the subcortex. Bars exceeding $|z| > 1$ (dashed horizontal lines) define the connectivity targets entered into the cluster-level aggregation step (see Methods); no inferential statistics are displayed in (**C**).

tests = 0.137), indicating greater aggregate FC in Montessori students compared to Traditional students. In addition, a Pedagogy × Age interaction emerged, F(1, 66) = 6.45, $p = 0.014$, pFDR-within-cluster = 0.034 (pFDR across all 25 tests = 0.166). Follow-up analyses indicated that the group difference increased with age, with Montessori-enrolled children showing a steeper age-related increase in FC in this cluster (i.e., a stronger positive association between age and FC, rather than a within-person longitudinal trajectory). The size of these effects (partial $\eta^2 = 0.111$ and. 089) approached the boundary of the smallest effect this study is powered to detect (see Sensitivity power analysis below). For Cluster 5, trends were observed for both the main effect of Pedagogy, F(1, 66) = 5.69, $p = 0.020$, pFDR-within = 0.082, and the Pedagogy × Age interaction, F(1, 66) = 4.75, $p = 0.033$, pFDR-within = 0.082, neither of which survived correction (Fig. 2B, C). For Cluster 8, a Pedagogy × Gender interaction was observed at



Fig. 2 | A Yeo's main network FC profiles per cluster. **B** Estimated marginal means by Pedagogy and Gender; the Cluster 2 main effect of Pedagogy shown here is significant under within-cluster FDR correction (pFDR = 0.027); under the more conservative across-25-test global FDR it does not reach significance (pFDR = 0.137) but the uncorrected p-value remains small ($p = 0.005$; see Table S7). **C** Age × Pedagogy associations per cluster; the increasing between-group divergence in Cluster 2 is significant under within-cluster FDR (pFDR = 0.034). Asterisks denote significance under the within-cluster FDR correction (the primary correction reported in the main text); ns denotes non-significant terms under either correction. Shaded bands in (**C**) show 95% confidence intervals from the GLM.

the uncorrected level, F(1, 66) = 4.55, $p = 0.037$, but did not remain significant after correction (pFDR-within = 0.163). No other main effects or interactions reached significance (ps_FDR > 0.25) in the other clusters. Full statistics under both correction schemes are reported in Table S3 and Table S7.

Robustness of the Cluster 2 effects. Four complementary checks indicate that the Cluster 2 Pedagogy main effect and Pedagogy × Age interaction are robust to plausible alternative specifications and to influential observations. First, adding head-motion covariates (FD, DVARS) to the GLM strengthened rather than weakened both effects (motion-adjusted Pedagogy: F(1, 61) = 7.70, $p = 0.007$, partial $\eta^2 = 0.112$; Pedagogy × Age: F(1, 61) = 5.73, $p = 0.020$, partial $\eta^2 = 0.086$; $N = 69$ motion-complete subjects). Second, nonparametric permutation tests with 10'000 re-labelings of Pedagogy yielded permutation p-values of 0.005 (Pedagogy) and. 009 (Pedagogy × Age), closely matching the parametric values. Third, in a leave-one-out analysis, the Cluster 2 Pedagogy × Age F-statistic remained above the parametric threshold (uncorrected $p < 0.05$) in 72/72 fits (range of F: 5.02–9.53), indicating that no single participant drives the effect. Fourth, a quadratic-age model in which Age² was added to the GLM left the linear Pedagogy × Age interaction essentially unchanged (F(1, 65) = 5.57, $p = 0.021$), with Age² itself contributing no significant variance ($F = 0.05$, $p = 0.83$). A nonparametric bootstrap 95% CI for the Pedagogy × Age coefficient was [+ 0.0025, + 0.0199], excluding zero. Full output is in Suppl. Table S11.

Discussion

Our data-driven parcellation and connectivity analyses suggest that thalamo-cortical organization in childhood is developmentally differentiated and varies by educational context in a cluster-specific manner. After evaluating multiple granularities, we retained the K = 8 solution because it maximized cluster compactness across different metrics as well as hemispheric symmetry while yielding functionally interpretable profiles for 5 clusters. The K = 7 solution, although aligned with several adult reports, included a spatially scattered cluster of low anatomical plausibility, whereas $K = 6$ reduced specificities. This pattern is compatible with age-related shifts in optimal parcellation grain (e.g., see ref. 20) and with elevated variability in network organization between ages 4–15[21], with early pediatric cohorts often favoring coarser solutions (e.g., $K = \sim 5$; see ref. 19) and adults finer ones (e.g., $K = \sim 7$). Because the K-determination was performed within a single cohort, the $K = 8$ solution should be regarded as cohort-specific until externally replicated in larger developmental samples (e.g., HCP-Development, ABCD, or the Healthy Brain Network); we view such cross-cohort validation as an essential next step but one that lies beyond the scope of the present analyses.

To contextualize the cluster-wise results, the $K = 8$ segmentation yielded dissociable, interpretable connectivity profiles across large-scale networks (Fig. 1C) that align with established thalamic-cortical motifs[22]. Cluster 1 coupled with the visual network and anticorrelated with limbic regions, consistent with pulvinar-linked sensory selection and visual-limbic dissociation[14,23,24]. Clusters 2 and 5 jointly engaged subcortical structures and the ventral attention network, a profile associated with salience detection and reorienting[25–27]. Within this set, Cluster 2 showed anticorrelation with dorsal attention, aligning with complementary bottom-up vs. top-down control[14,23,28–31]. Cluster 5 showed concurrent anticorrelations with visual and limbic networks, a pattern consistent with balancing exteroceptive input and internal emotional context[32]. By contrast, Cluster 4 preferentially coupled with somatomotor and dorsal attention networks and anticorrelated with limbic regions, matching ventrolateral/ventroanterior motor thalamus involvement in sensorimotor-attentional integration[1,33–36]. Collectively, these connectivity profiles support a view of the pediatric thalamus as a set of specialized modulatory units rather than a unitary hub.

Within this parcellation, several clusters displayed associations with pedagogy, age, and gender. These associations are correlational and arise from a cross-sectional, self-selected sample. The most robust effect localized to Cluster 2 (subcortical/ventral-attention coupling with dorsal-attention anticorrelation): Montessori enrollment was associated with stronger functional coupling (F(1,66) = 8.26, pFDR = 0.027), and the between-group difference increased with age (Pedagogy × Age: F(1,66) = 6.45, pFDR = 0.034). A similar, uncorrected trend appeared for Cluster 5 (dorsal attention-somatomotor), where trajectories differed by pedagogy (decreasing FC with age in traditionally schooled children, increasing in Montessori). These associations are compatible with the idea that classroom experiences co-vary with thalamic channels implicated in salience and sensorimotor–attentional integration, but they do not establish directional effects. In a sensitivity analysis restricted to the 35 children for whom years-in-current-school was available, time-in-pedagogy did not predict aggregate FC in Cluster 2 (F(1,28) = 0.01, $p = 0.92$) and the Pedagogy and Pedagogy × Age terms remained significant (ps = 0.012 and. 032; Suppl. Table S6), arguing against a simple cumulative-dose interpretation but not ruling out unmeasured family-level differences such as parental endorsement of pedagogical values, prior schooling history, or home learning environment. We also observed a Pedagogy × Gender interaction in Cluster 8 (ventral thalamus) at the uncorrected level (F(1,66) = 4.55, $p = 0.037$; pFDR = 0.163): gender differences were evident in the traditional group and not apparent in the Montessori group. Given correction thresholds and sample size, this pattern should be considered provisional and hypothesis-generating.

Absences were informative. Across solutions, resting-state thalamic coupling with default-mode (DMN) and executive-control (ECN) networks was not prominent. Adult work often reports thalamo-DMN and thalamo-prefrontal interactions[1,34] whereas DMN specialization and ECN integration strengthen later in development [21,35]. The present pattern is consistent with this timetable and with stronger thalamic links to sensorimotor and attention systems in childhood[36]. Future task-based studies could test whether DMN/ECN-related thalamic interactions emerge under cognitive load despite weak resting-state associations.

Methodologically, three features strengthen interpretability. First, the parcellation was data-driven and pediatric-adapted, with the choice of K guided by a priori anatomical and functional criteria rather than adult atlas transfer. Second, clusters with low voxel counts or poor spatial coherence were excluded to prioritize biological plausibility. Third, effects were estimated at the cluster level rather than collapsed across the thalamus, respecting known heterogeneity. Still, several limitations circumscribe inference. The design is cross-sectional; thus, associations between pedagogy and connectivity cannot be interpreted as directional influences. Data were collected between 2018 and 2021; newer multiband acquisitions and denoising approaches (e.g., field map inclusion) could further improve small-nuclei fidelity. Resting-state measures may underestimate condition-dependent dynamics; tasks probing exogenous orienting, set reconfiguration, and affective conflict could provide complementary tests. Several interactions (e.g., Pedagogy × Gender in Cluster 8; Cluster 5 trends) did not survive correction and warrant confirmation in larger, preregistered samples. The headline Cluster 2 effects survive the within-cluster FDR (the primary correction reported in the main text) but not the more conservative across-25-test FDR (Table S7); we therefore present these as robust exploratory findings pending independent replication. A sensitivity power analysis (Suppl. Table S8) indicates the study is powered ($1\text{-}\beta = 0.80$, $\alpha = 0.05$) to detect effects of Cohen's $f^2 = \sim 0.12$ and above (partial $\eta^2 = \sim 0.11$); null effects in the other clusters should therefore not be interpreted as evidence of absence of smaller true effects. Importantly, beyond SES, which was matched at the group level, additional family-level covariates that may differentiate Montessori- and traditionally-schooled families (parental endorsement of pedagogical values, parental education, prior schooling history, child-driven self-selection, home learning environment, child temperament) were not fully controlled. Although time-in-current-school did not account for the Cluster 2 effects in the subset for which it was available, residual confounding from these unmeasured dimensions cannot be excluded. The within-cluster FDR correction we adopt as the primary inference rests on a specific design feature: the five thalamic territories were defined by an entirely unsupervised data-driven parcellation step that is blind to Pedagogy, Age, and Gender, and each territory exhibits a distinct,

theoretically motivated cortical-network connectivity profile (Fig. 1C). Each cluster therefore constitutes a separable biological hypothesis with a different putative function; the five clusters are conceptually independent outcomes. Under this view, applying Benjamini–Hochberg within each cluster (across the five GLM effects that share that outcome) is the appropriate correction. The more conservative across-25-test correction is reported alongside for transparency (Table S7).

By combining pediatric data-driven thalamic mapping with variation in real-world educational environments, the present study identifies selective associations between schooling context and the maturation of thalamocortical circuits supporting attention and sensorimotor integration. Rather than reflecting global differences in brain organization, these effects appear localized to specific attention-related thalamic channels, consistent with models in which the thalamus dynamically regulates information flow across cortical networks during learning. These findings suggest that everyday learning environments may relate to the developmental refinement of neural systems that prioritize and route information during cognition. Longitudinal designs (within-person, ideally with cross-pedagogy switchers) and experimental or quasi-experimental approaches will be necessary to move beyond association and determine whether educational experiences contribute causally to these age-related differences in thalamocortical organization.

Methods

Participants

This study is part of an ongoing longitudinal investigation (initiated in 2018) examining how school environments shape neurocognitive development in childhood. Participants were recruited from either Montessori or traditional school systems within the region, with similar time spent in each settings (see Table S10). Inclusion criteria required active enrollment in one of these educational settings. Children with reported learning disabilities or developmental disorders, as disclosed by parents or legal guardians, were excluded. All procedures were approved by the local ethics committee (Commission d'Ethique Romande CER-VD 2018-00244) and conducted in accordance with the Declaration of Helsinki. Written informed consent was obtained from legal guardians, and verbal assent was provided by all participating children. Participation was voluntary, and children were free to withdraw at any time without consequence. As compensation, participants received a gift voucher.

Ninety-six children had available resting-state functional MRI (rs-fMRI) data. We restricted the sample to participants aged 4–15 years (M = 9.78, SD = 2.58), resulting in the exclusion of 6 individuals outside this range. Following rigorous quality control procedures (see Neuroimaging Preprocessing section), 18 additional participants were excluded due to incomplete imaging data (e.g., presence of dental braces, $n = 1$) or excessive head motion during scanning ($n = 17$). The final sample comprised 72 participants (see Table 1 for demographics and group distributions).

Behavioral measures and demographics

All behavioral data were collected on the day of the MRI scan. Children completed assessments either before or after imaging in a quiet room, under the supervision of an experimenter. Variables included for this study were chronological age, gender, and fluid intelligence, measured using Raven's Progressive Matrices PM47[37]. While children were in the scanner, parents or guardians completed questionnaires assessing, among others, socioeconomic status (SES; see ref. 38) and interest in pedagogical practices based on a tailor-made questionnaire. These additional measures served to identify and control for potential confounding variables, especially important given that Montessori school enrollment is often associated with higher SES backgrounds[15].

All data were anonymized and checked for accuracy and completeness prior to analysis. Missing values were rare and confined to a small number of behavioural-questionnaire items (<5% of cells per affected variable). For the demographic variables used as covariates in the present report (age, gender, SES, fluid intelligence), no values were missing; consequently, no imputation was performed for the variables entering the GLM analyses. For the supplementary covariate analysis using time-in-current-school (years_school; see Section 'Sensitivity analyses'), this variable was available for 35 of 72 children, and analyses including it were therefore restricted to that subsample without imputation.

Statistical Analysis of Behavioral Measures and Demographics

Group differences in age, SES, and fluid intelligence were assessed using independent samples t-tests. Gender distribution and parental interest for pedagogy were compared via chi-square analysis. All statistical analyses were conducted using jamovi (v. 2.6; https://www.jamovi.org).

Neuroimaging Acquisition

All MRI data were acquired on a 3 T Siemens Prisma-Fit scanner (VE11E) with a 64-channel head coil at the University Hospital. Structural images used a 3D T1-weighted MP-RAGE sequence (sagittal; TR/TE/TI = 2000/2.47/900 ms; flip angle = 8°; FOV = 256 × 256 mm^2; voxel size = 1 × 1 × 1 mm^3). Resting-state fMRI consisted of a 6 min multiband EPI run (720 volumes; TR = 500 ms; TE = 33 ms; flip angle = 80°; 48 contiguous axial slices; multiband factor = 8; matrix = 94 × 94; FOV = 224 × 224 mm^2; bandwidth = 2418 Hz/Px; EPI factor = 94), yielding 2.4 mm isotropic voxels. To limit motion, foam padding stabilized the head. During the rs-fMRI, participants kept their eyes open, fixated a central cross, remained still, and let their minds wander without falling asleep.

Neuroimaging preprocessing

Image preprocessing and quality control were performed using fMRIPrep 20.2.1[39], a robust pipeline based on Nipype 1.5.1[40]. The preprocessing pipeline included skull stripping, intensity normalization, bias field correction, motion correction, coregistration to T1-weighted anatomical scans, and normalization to standard MNI space (MNI152NLin2009cAsym).

To account for potential confounding effects of head motion, we included both automated and manual quality control procedures. Functional MRI quality was evaluated using FD and DVARS metrics[41]. Participants were excluded if their mean FD exceeded 0.5 mm, if DVARS indicated excessive signal variability, or if there were visible artifacts (e.g., due to dental implants or failed anatomical-functional registration). To examine whether residual motion varied systematically by demographic or experimental factors, we conducted separate ANOVAs on FD and DVARS with Pedagogy, Age, and Gender as predictors (excluding higher-order three-way interactions). Results indicated no significant effects of pedagogy, age, or gender on DVARS (all ps > 0.46; Table S1). In contrast, FD was marginally lower with increasing age ($F(1,63) = 4.29$, $p = 0.043$) but was not influenced by pedagogy or gender (Table S2). These findings support the interpretation that group-level differences in functional connectivity are unlikely to be driven by systematic motion artifacts.

Thalamic clustering procedure using KNIT model

Functional parcellation of the thalamus was performed using an adaptation of the KNIT (K-means for Nuclei in Infants' Thalamus) model[19], originally developed for neonatal populations. All analyses were implemented in Python (PyCharm 2025.1.1.1).

Anatomical regions were defined according to the Lausanne2018 parcellation (508 ROIs, scale 3, comprising 448 cortical and 60 subcortical/cerebellar regions) as implemented in Connectome Mapper v3[42]; the T1 parcellation was rigidly registered to each participant's averaged resting-state BOLD image using ITK-SNAP[43]. A thalamic mask was generated per subject based on the parcellation. Then, functional connectivity (FC) was computed between each thalamic voxel and all parcels of the Lausanne2018-508 atlas (cortex+subcortex) by correlating voxel time series with parcel-wise mean time series. This produced individual voxel-wise FC maps. These individual maps were then Fisher z-transformed to normalize correlation values and averaged across the full cohort to generate a population-level thalamic FC map. A mean thalamic mask was derived from this group map, retaining only voxels for which the group-level mean absolute Fisher-z

connectivity exceeded the 10th percentile of the within-mask distribution and which were present in ≥90% of individual subject masks (consistency criterion). This step excluded <8% of original thalamic-mask voxels and improved signal specificity.

To identify distinct functional territories within the thalamus, the resulting group-level FC maps were submitted to k-means clustering. Each thalamic voxel was assigned to one of K clusters based on the similarity of its whole-brain connectivity profile. Clustering was conducted iteratively across a broadened range of values ($K = 3$ to $K = 15$) to evaluate segmentation stability and functional interpretability. This range encompassed both lower-order solutions (consistent with neonatal parcellations; see ref. 19) and finer solutions (consistent with adult anatomical subdivisions; see ref. 9). For each K, we computed three complementary cluster-quality metrics: (i) the silhouette coefficient, (ii) the Calinski–Harabasz index, and (iii) the Davies–Bouldin index. We additionally quantified the bilateral symmetry of each clustering solution as the Adjusted Rand Index (ARI) between the left- and right-hemisphere parcellations[20,44]. The combination of quantitative indices and a priori anatomical/functional criteria (spatial coherence, hemispheric symmetry, and functional specificity) was used to guide the final choice of K. Detailed metrics for $K = 3$ to 15 are reported in Suppl. Figure S5.

Cluster validation and network characterization

The functional connectivity profile of each thalamic cluster was characterized by examining its whole-brain connectivity pattern in relation to the canonical seven-network cortical parcellation proposed by Yeo et al. [45,46]. Connectivity values were Fisher z-transformed to normalize the distribution and then thresholded for visualization to highlight networks showing strong positive connectivity ($z > +1$) or strong negative connectivity / anticorrelation ($z < -1$). For the subsequent voxel-wise screening step, networks reaching $z > +1$ or $z < -1$ in the group mean were carried forward into the cluster-level aggregation; this is the criterion referred to throughout the manuscript as 'previously identified as significant in the voxel-wise analysis'.

Clustering solutions were systematically evaluated according to three criteria: spatial coherence (including bilateral symmetry and compactness), functional specificity (defined by the distinctiveness of each cluster's cortical connectivity signature), and anatomical plausibility (cluster size and topography). The 60-voxel exclusion threshold corresponded to approximately 3% of the total thalamic volume in our cohort (i.e., the smallest size at which a bilateral, spatially coherent micro-territory can plausibly be sustained at 2.4 mm isotropic resolution; cf. minimum-size conventions used in refs. 9, 20) and was decided a priori, before model selection. Sensitivity analyses retaining the small clusters and Cluster 7 (108 voxels), which appeared spatially scattered and asymmetric on visual inspection, are reported in Suppl. Tables S5 and S5b; including or excluding these clusters did not alter the pattern of Pedagogy or Pedagogy × Age effects in the five interpretable territories.

Functional connectivity analyses

Functional connectivity (FC) values were aggregated within each thalamic cluster by averaging connectivity to the Yeo-network targets whose group-mean Fisher-z exceeded $|z| > 1$ in the voxel-wise screening described above (i.e., the same threshold used to define the cluster fingerprints in Fig. 1C; e.g., Visual, Limbic). Separate general linear models were estimated for each cluster with Pedagogy (Traditional vs. Montessori; between-subject), Gender (Male vs. Female; between-subject), and Age (continuous, in years) as predictors. The full model included Pedagogy × Age and Pedagogy × Gender interactions. The Age × Gender and three-way Pedagogy × Age × Gender terms were excluded from the planned model to preserve degrees of freedom given $N = 72$: gender is not theorized to interact with age in the present hypothesis space, and a three-way interaction was a priori unlikely to be detectable at this sample size (see Sensitivity analyses and Table S6 for a confirmatory model that re-introduces both terms). Models were evaluated with Type III ANOVAs using the car package in R.

For post hoc inference, estimated marginal means were obtained via the emmeans package. Because each thalamic territory has a distinct functional fingerprint and was tested against an independent set of theoretically motivated effects, our primary correction was an FDR applied within each cluster across its five effects (Benjamini–Hochberg). To address the more conservative concern that all 25 tests should be jointly corrected, we also report a sensitivity analysis in which Benjamini–Hochberg FDR is applied across the full $5 \times 5 = 25$ test family (Table S7). Data visualization was performed with ggplot2 and patchwork.

To further ensure that observed FC differences were not confounded by residual motion artifacts, we conducted a control analysis on global mean FC including FD and DVARS as covariates. Neither motion metric explained significant variance in FC (both FDR-adjusted ps > 0.70), indicating minimal influence of head motion on the main findings (Fig. S1).

Sensitivity analyses

We ran four planned sensitivity models in addition to the main GLM: (i) re-fitting each cluster model after applying Benjamini-Hochberg FDR across the full 5 clusters × 5 effects = 25-test family (Table S7); (ii) re-fitting the Cluster 2 model after iteratively removing the oldest participants (age ≤ 13, ≤ 12, ≤ 11 years) to confirm that the Pedagogy × Age interaction is not driven by the upper tail of the age distribution (Table S5); (iii) re-fitting the Cluster 2 and Cluster 5 models in the subsample of children for whom time-in-current-school was available, with years_school added as a continuous covariate (Table S6); and (iv) re-fitting all cluster models with the full crossed Pedagogy × Age × Gender model that includes the previously dropped Age × Gender and three-way interactions (Table S6b).

Because Cluster 2 carries the main inferential weight of the paper, we ran four additional, post hoc robustness checks on this cluster: (a) a motion-adjusted GLM that adds mean framewise displacement (FD) and DVARS as covariates in the main model ($N = 69$ motion-complete subjects); (b) permutation tests of the Pedagogy and Pedagogy × Age effects, with 10,000 random re-labelings of Pedagogy across subjects (full $N = 72$); (c) a leave-one-out analysis in which each subject is dropped in turn and the Cluster 2 Pedagogy × Age F-statistic is recomputed; and (d) a quadratic-age sensitivity in which Age^2 is added to the model to test whether the linear Pedagogy × Age interaction is an artifact of nonlinearity. We also report a nonparametric bootstrap 95% CI (10'000 resamples) for the Cluster 2 Pedagogy × Age coefficient. Results are reported in Suppl. Table S11.

For the planned model (one intercept + five predictor terms, residual df = 66 at $N = 72$), a one-degree-of-freedom F-test attains 80% power at $\alpha = 0.05$ to detect effects of Cohen's $f^2 = \sim 0.12$ (partial $\eta^2 = \sim 0.107$) and above, and a two-degree-of-freedom test attains 80% power for $f^2 = \sim 0.15$. The observed Cluster 2 Pedagogy and Pedagogy × Age effects (partial $\eta^2 = 0.111$ and 0.089) lie close to this boundary; null effects in the other clusters should therefore be interpreted with this minimum-detectable-effect-size in mind. Full effect sizes for every term are reported in Suppl. Table S8.

Data availability

All analysis scripts and preprocessed data supporting the findings of this study will be made publicly available on a GitLab repository upon publication.

Code availability

All analysis scripts of this study will be made publicly available on a GitLab repository upon publication.

Received: 30 March 2026; Accepted: 20 August 2026;
Published online: 03 September 2026

References

1. Hwang, K., Bertolero, M. A., Liu, W. B. & D'Esposito, M. The human thalamus is an integrative hub for functional brain networks. *J. Neurosci.* **37**, 5594–5607 (2017).

2. Shine, J. M., Lewis, L. D., Garrett, D. D. & Hwang, K. The impact of the human thalamus on brain-wide information processing. *Nat. Rev. Neurosci.* **24**, 416–430 (2023).
3. de Bourbon-Teles, J. et al. Thalamic control of human attention driven by memory and learning. *Curr. Biol.* **24**, 993–999 (2014).
4. Hwang, K., Shine, J. M., Cole, M. W. & Sorenson, E. Thalamocortical contributions to cognitive task activity. *eLife* **11**, e81282 (2022).
5. Bandiera, S. & Molnár, Z. Development of the thalamocortical systems. In *The Thalamus* (ed. Halassa, M. M.) 139–162 (Cambridge Univ. Press, Cambridge, 2022).
6. Wolff, M., Morceau, S., Folkard, R., Martin-Cortecero, J. & Groh, A. A thalamic bridge from sensory perception to cognition. *Neurosci. Biobehav. Rev.* **120**, 222–235 (2021).
7. Guillery, R. W. Anatomical evidence concerning the role of the thalamus in corticocortical communication: a brief review. *J. Anat.* **187**, 583–592 (1995).
8. Li, Y. et al. Distinct subnetworks of the thalamic reticular nucleus. *Nature* **583**, 819–824 (2020).
9. Najdenovska, E. et al. In-vivo probabilistic atlas of human thalamic nuclei based on diffusion-weighted magnetic resonance imaging. *Sci. Data* **5**, 180270 (2018).
10. Nakajima, M. & Halassa, M. M. Thalamic control of functional cortical connectivity. *Curr. Opin. Neurobiol.* **44**, 127–131 (2017).
11. Wells, M. F., Wimmer, R. D., Schmitt, L. I., Feng, G. & Halassa, M. M. Thalamic reticular impairment underlies attention deficit in Ptchd1(Y/-) mice. *Nature* **532**, 58–63 (2016).
12. Ivanov, I. et al. Morphological abnormalities of the thalamus in youths with attention deficit hyperactivity disorder. *Am. J. Psychiatry* **167**, 397–408 (2010).
13. Müller-Axt, C., Kauffmann, L., Eichner, C. & von Kriegstein, K. Dysfunction of the magnocellular subdivision of the visual thalamus in developmental dyslexia. *Brain* **147**, 4283–4297 (2024).
14. Halassa, M. M. & Kastner, S. Thalamic functions in distributed cognitive control. *Nat. Neurosci.* **20**, 1669–1679 (2017).
15. Marshall, C. Montessori education: a review of the evidence base. *npj Sci. Learn.* **2**, 11 (2017).
16. Denervaud, S., Gentaz, E., Matusz, P. J. & Murray, M. M. Multisensory gains in simple detection predict global cognition in schoolchildren. *Sci. Rep.* **10**, 1394 (2020).
17. Denervaud, S., Mumaw, J. T., Gentaz, E. & Murray, M. M. Multisensory perception in schoolchildren with neurodevelopmental disorders: links with academic performance and adaptive behavior. *Trends Neurosci. Educ.* **25**, 100165 (2021).
18. Zanchi, P. et al. Differences in spatiotemporal brain network dynamics of Montessori and traditionally schooled students. *npj Sci. Learn.* **9**, 45 (2024).
19. Kebiri, H., Delavari, F., Van De Ville, D., Jorge, J. & Cuadra, B. ach M. Functional organization of the neonatal thalamus across development depicted by functional MRI. *Imaging Neurosci* **3**, IMAG-a-87 https://doi.org/10.1162/IMAG.a.87 (2025).
20. Fan, Y. et al. Functional connectivity-based parcellation of the thalamus: an unsupervised clustering method and its validity investigation. *Brain Connect* **5**, 620–630 (2015).
21. Fair, D. A. et al. Maturing thalamocortical functional connectivity across development. *Front. Syst. Neurosci.* **4**, 10 (2010).
22. Segobin, S. et al. A roadmap towards standardized neuroimaging approaches for human thalamic nuclei. *Nat. Rev. Neurosci.* **25**, 792–808 (2024).
23. Saalmann, Y. B., Pinsk, M. A., Wang, L., Li, X. & Kastner, S. The pulvinar regulates information transmission between cortical areas based on attention demands. *Science* **337**, 753–756 (2012).
24. Arcaro, M. J., Pinsk, M. A. & Kastner, S. The anatomical and functional organization of the human visual pulvinar. *J. Neurosci.* **35**, 9848–9871 (2015).
25. Corbetta, M. & Shulman, G. L. Control of goal-directed and stimulus-driven attention in the brain. *Nat. Rev. Neurosci.* **3**, 201–215 (2002).
26. Corbetta, M. & Shulman, G. L. Spatial neglect and attention networks. *Annu. Rev. Neurosci.* **34**, 569–599 (2011).
27. Vossel, S., Geng, J. J. & Fink, G. R. Dorsal and ventral attention systems. *Neuroscientist* **20**, 150–159 (2014).
28. Fox, M. D., Corbetta, M., Snyder, A. Z., Vincent, J. L. & Raichle, M. E. Spontaneous neuronal activity distinguishes human dorsal and ventral attention systems. *Proc. Natl Acad. Sci. USA* **103**, 10046–10051 (2006).
29. Zhou, H., Schafer, R. J. & Desimone, R. Pulvinar-cortex interactions in vision and attention. *Neuron* **89**, 209–220 (2016).
30. Kragel, P. A. et al. A human colliculus-pulvinar-amygdala pathway encodes negative emotion. *Neuron* **109**, 2404–2412.e5 (2021).
31. Mitchell, A. S. The mediodorsal thalamus as a higher order thalamic relay nucleus important for learning and decision-making. *Neurosci. Biobehav. Rev.* **54**, 76–88 (2015).
32. Cortes, N., Ladret, H. J., Abbas-Farishta, R. & Casanova, C. The pulvinar as a hub of visual processing and cortical integration. *Trends Neurosci* **47**, 120–134 (2024).
33. Sherman, S. M. & Guillery, R. W. Functional organization of thalamocortical relays. *J. Neurophysiol.* **76**, 1367–1395 (1996).
34. Schmitt, L. I. et al. Thalamic amplification of cortical connectivity sustains attentional control. *Nature* **545**, 219–223 (2017).
35. Satterthwaite, T. D. et al. Functional maturation of the executive system during adolescence. *J. Neurosci.* **33**, 16249–16261 (2013).
36. Park, S. et al. A shifting role of thalamocortical connectivity in the emergence of cortical functional organization. *Nat. Neurosci.* **27**, 1609–1619 (2024).
37. Raven, J. C., Raven, J. & Court, J. H. *Manual for Raven's Progressive Matrices and Vocabulary Scales* (Pearson Education, London, 1998).
38. Genoud, P. A. *Indice de position socio-économique (IPSE): un calcul simplifié* (Université de Fribourg, Fribourg, 2011).
39. Esteban, O. et al. fMRIPrep: a robust preprocessing pipeline for functional MRI. *Nat. Methods* **16**, 111–116 (2019).
40. Gorgolewski, K. et al. Nipype: a flexible, lightweight and extensible neuroimaging data processing framework in Python. *Front. Neuroinform.* **5**, 13 (2011).
41. Power, J. D., Barnes, K. A., Snyder, A. Z., Schlaggar, B. L. & Petersen, S. E. Spurious but systematic correlations in functional connectivity MRI networks arise from subject motion. *Neuroimage* **59**, 2142–2154 (2012).
42. Tourbier, S. et al. Connectome Mapper 3: a flexible and open-source pipeline software for multiscale multimodal human connectome mapping. *J. Open Source Softw.* **7**, 4248 https://doi.org/10.21105/joss.04248 (2022).
43. Yushkevich, P. A. et al. User-guided 3D active contour segmentation of anatomical structures: significantly improved efficiency and reliability. *NeuroImage* **31**, 1116–1128 (2006).
44. Kahnt, T., Chang, L. J., Park, S. Q., Heinzle, J. & Haynes, J.-D. Connectivity-based parcellation of the human orbitofrontal cortex. *J. Neurosci.* **32**, 6240–6250 (2012).
45. Yeo, B. T. T. et al. The organization of the human cerebral cortex estimated by intrinsic functional connectivity. *J. Neurophysiol.* **106**, 1125–1165 (2011).
46. Lillard, A. S. Montessori: The Science Behind the Genius 3rd edn (Oxford Univ. Press, New York, 2017).

Acknowledgements

This work was supported by grants from the Swiss National Science Foundation (grants 182602, 215641) and the Société Académique Vaudoise. Imaging was supported in part by the Centre d'Imagerie Biomédicale (CIBM) of the Université de Lausanne (UNIL), Université de Genève (UNIGE), Hôpitaux Universitaires de Genève (HUG), Centre Hospitalier Universitaire Vaudois (CHUV), Ecole Polytechnique Fédérale de

Lausanne (EPFL), and the Leenaards and Jeantet Foundations. The funding sources had no role in study design, data collection, analysis, interpretation, or the decision to submit the manuscript.

Author contributions

S.D., M.B.C., H.K. designed the study, H.K. adjusted the pipeline, T.M.M, H.K., S.D., analyzed the data and wrote the main manuscript text. All authors reviewed the manuscript.

Competing interests

The authors declare no competing interests.

Additional information

Supplementary information The online version contains supplementary material available at https://doi.org/10.1038/s41539-026-00452-4.

Correspondence and requests for materials should be addressed to Solange Denervaud.

Reprints and permissions information is available at http://www.nature.com/reprints

Publisher's note Springer Nature remains neutral with regard to jurisdictional claims in published maps and institutional affiliations.

Open Access This article is licensed under a Creative Commons Attribution 4.0 International License, which permits use, sharing, adaptation, distribution and reproduction in any medium or format, as long as you give appropriate credit to the original author(s) and the source, provide a link to the Creative Commons licence, and indicate if changes were made. The images or other third party material in this article are included in the article's Creative Commons licence, unless indicated otherwise in a credit line to the material. If material is not included in the article's Creative Commons licence and your intended use is not permitted by statutory regulation or exceeds the permitted use, you will need to obtain permission directly from the copyright holder. To view a copy of this licence, visit http://creativecommons.org/licenses/by/4.0/.

© The Author(s) 2026

This Article in Press is shared early to give you faster access to new research. It is citable and carries a permanent DOI. The final edited version will replace it automatically.